Magnetic Compounds

DOI: 10.1002/ange.200501987

Hysteretic Magnetic Bistability Based on a Molecular Azide Switch**

*Guido Leibeling, Serhiy Demeshko, Sebastian Dechert, and Franc Meyer**

Dedicated to Professor Gottfried Huttner on the occasion of his 68th birthday

Materials that exhibit hysteretic bistability at temperatures not too far from ambient conditions are expected to have great potential for future memory or sensing applications.[1] The two relatively stable states should be clearly distinguished by their physical properties, such as their magnetic or optical characteristics. Thermal magnetic hysteresis with an abrupt and rapid property change around room temperature is particularly rare for molecule-based materials,[2] with spin-crossover compounds providing the most prominent examples.[3] More recently, magnetic hysteresis has also been observed for some molecular organic radicals[4] or transition metal coordination compounds,[5,6] where switching between two states occurs through a thermal phase transition with orientational changes in the 3D crystal lattice. Herein, we report thermal hysteresis of the magnetic susceptibility for single crystals of the molecular dinickel(II) complex $[LNi_2(N_3)_3]$ (**1**), in which a $\mu_{1,3}$-azido ligand functions as an on/off switch for the intramolecular antiferromagnetic coupling between the two metal ions.

Pyrazolate-based compartmental ligands such as L^-, which bears thioether side-arms, have previously proven suitable as dinucleating scaffolds for the synthesis of preorganized azidonickel(II) complexes that can serve as modules for the assembly of oligonuclear species or 1D extended chain compounds;[7] the bimetallic complex **1** was prepared as a potential building block in this context. Single crystals of **1** were grown from acetone/hexane, and an initial X-ray crystallographic analysis was carried out at 133 K (Figure 1).[8] As anticipated, both nickel ions in the C_2-symmetric array are nested within their respective ligand compartment (with two sulfur and one nitrogen donors from the ligand side-arm) and are spanned by the bridging pyrazolate. A $\mu_{1,3}$-azido bridge is found within the bimetallic pocket, and an additional terminal azide fills the remaining site at each of the six-coordinate metal ions.

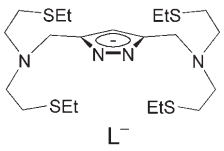

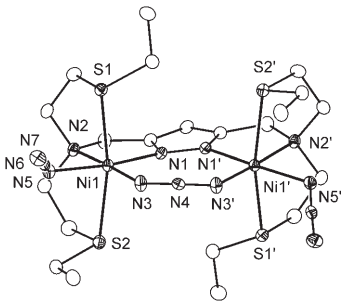

Figure 1. ORTEP plot (30% probability thermal ellipsoids) of the structure of **1** at 133 K. All hydrogen atoms have been omitted for the sake of clarity.

Since **1** did not exhibit any unusual structural features at this stage, the temperature dependence of its magnetic susceptibility was highly unexpected. The product $\chi_M T$ for a polycrystalline sample of **1** is depicted in Figure 2 for both decreasing and increasing temperature. The value of $1.82\ cm^3 K mol^{-1}$ at 300 K is somewhat lower then the spin-only value expected for two uncoupled high-spin nickel(II) ions ($2.14\ cm^3 K mol^{-1}$ for $g = 2.07$), and decreases only slightly upon lowering the temperature to 220 K. At 215 K, however, an abrupt drop of $\chi_M T$ occurs (centered at $T_\downarrow = 212$ K), followed by a much more rapid decline at lower temperatures; below 50 K $\chi_M T$ tends towards zero. The low-temperature data are indicative of strong antiferromagnetic coupling and an $S = 0$ ground state, while coupling is apparently only weak above 220 K. $\chi_M T$ shows an analogous behavior when measured as a function of increasing temperature, but exhibits thermal hysteresis with $\Delta T \approx 13$ K ($T_\uparrow$

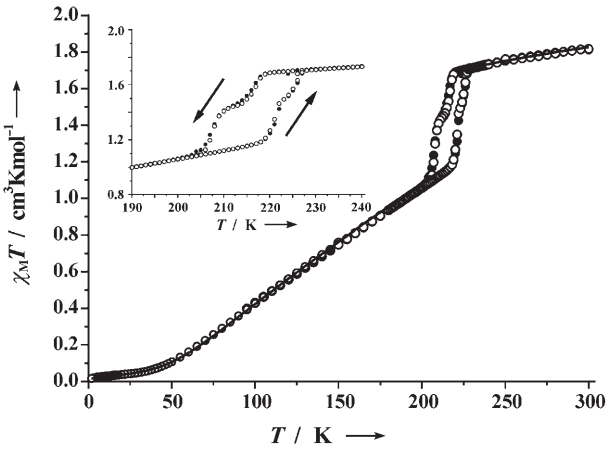

Figure 2. Plot of $\chi_M T(T)$ at two different magnetic fields (closed circles: 5000 G; open circles: 2000 G) for decreasing and increasing temperature. The solid lines represent the calculated curve fits at high and low temperature (see text). The inset shows an enlargement for the temperature region between 190 und 240 K.

[*] Dr. G. Leibeling, S. Demeshko, Dr. S. Dechert, Prof. Dr. F. Meyer
Institut für Anorganische Chemie
Georg-August-Universität Göttingen
Tammannstrasse 4, 37077 Göttingen (Germany)
Fax: (+49) 551-39-3063
E-mail: franc.meyer@chemie.uni-goettingen.de

[**] Financial support from the DFG (priority program 1137 "Molecular Magnetism") is gratefully acknowledged.

Supporting information for this article is available on the WWW under http://www.angewandte.org or from the author.

centered at 223 K). No field dependence of the magnetic data was observed. Complex **1** thus undergoes a reversible and field-independent switching of the magnitude of the magnetic exchange interaction, with hysteresis occurring not too far from room temperature.

The experimental magnetic data were modeled separately in the range from 200 to 5 K and above 230 K using Equation (1), which is deduced from the Hamiltonian $\mathscr{H} = -2J\hat{S}_1\hat{S}_2$, with additional terms accounting for residual amounts of paramagnetic impurity (ρ), and for the temperature-independent paramagnetism (TIP).

$$\chi_M = \frac{N g^2 \mu_B^2}{k T}\frac{2e^{2(J/kT)} + 10e^{6(J/kT)}}{1 + 3e^{2(J/kT)} + 5e^{6(J/kT)}}(1-\rho) + \frac{2N g^2 \mu_B^2}{3kT}\rho + \mathrm{TIP} \qquad (1)$$

Good fits were obtained with the parameters $g = 2.24 \pm 0.01$, $J = -(81 \pm 1.5)\ \mathrm{cm}^{-1}$ ($\rho = (0.6 \pm 0.1)\%$; $\mathrm{TIP} = 1.2 \times 10^{-3}$) at low temperatures and $g = 2.07 \pm 0.01$, $J = -(24 \pm 1.0)\ \mathrm{cm}^{-1}$ ($\rho = (0.8 \pm 0.1)\%$; $\mathrm{TIP} = 1.0 \times 10^{-4}$) above 230 K,[9] thereby confirming the drastic differences in the strength of the antiferromagnetic coupling for the two temperature domains, with strong or weak antiferromagnetic coupling below or above the hysteretic transition, respectively.

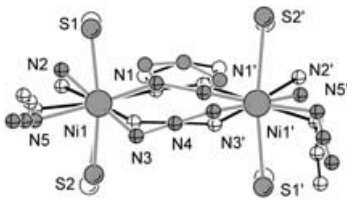

Figure 3. Overlay of the molecular structures at 253 K (grey) and 133 K (white) of **1**, showing the changes of the dihedral angles. Selected interatomic distances [Å] and angles [°] at 133 K [253 K]: Ni1-N1 2.071(3) [2.065(2)], Ni1-N2 2.139(3) [2.136(3)], Ni1-N3 2.056(3) [2.078(3)], Ni1-N5 2.079(3) [2.067(3)], Ni1-S1 2.4279(9) [2.436(1)], Ni1-S2 2.5319(9) [2.496(1)], Ni1···Ni1′ 4.5538(8) [4.5201(8)], N3-N4 1.174(3) [1.170(3)]; N1-Ni1-N5 170.6(1) [171.2(1)], N2-Ni1-N3 177.3(1) [178.4(1)], S1-Ni1-S2 167.96(3) [169.26(4)], N1-Ni1-N2 82.6(1) [82.3(1)], N2-Ni1-N5 88.7(1) [88.9(1)], N5-Ni1-N3 91.4(1) [92.7(1)], N3-Ni1-N1 97.5(1) [96.1(1)], N4-N3-Ni1 120.7(3) [116.7(3)], N3-N4-N3′ 176.4(5) [177.5(5)]. Symmetry transformation used to generate equivalent atoms (′): $1-x$, y, $1.5-z$.

Table 1: Unit-cell parameters and selected dihedral angles for **1** at different temperatures.

T [K]	a [Å]	b [Å]	c [Å]	V [Å^3]	Ni1-N1-N1′-Ni1′ [°]	Ni1-N3-N3′-Ni1′ [°]
133	15.9739(12)	8.6167(8)	22.8983(17)	3151.8(4)	23.1(6)	4.3(4)
195	16.0886(12)	8.6241(8)	22.9437(16)	3183.4(4)	20.9(7)	4.8(5)
223	16.3424(12)	8.6933(8)	22.9634(15)	3262.4(4)	−39.8(7)	−48.7(4)
253	16.3677(10)	8.7169(7)	22.9876(13)	3279.8(4)	−38.8(6)	−46.6(4)

In order to elucidate the molecular cause of this unexpected magnetic behavior and to characterize the magnetic phase transition, a single crystal of **1** was investigated crystallographically at different temperatures. The crystal was first mounted at room temperature and data sets were then collected at 253, 173, 223, and 195 K (in that order). In each case the temperature was allowed to equilibrate for one hour before data collection was started. It is apparent from the crystallographic data that the crystal stays intact upon temperature variation and repeated shuttling through the hysteresis range as the crystal system remains orthorhombic for all temperatures. Inspection of the molecular structures above and below the hysteresis temperature, however, reveals significant differences of the bimetallic scaffold. These differences can clearly be seen by overlaying the molecular structures of the central dinickel core obtained at 133 and 253 K (Figure 3).

Structural alterations are basically expressed through changes of the dihedral angle formed by the two metal centers and the outer nitrogen atoms of the bridging azide (N3 and N3′) as well as the dihedral angle formed by the metals and the pyrazolate nitrogen atoms (N1 and N1′) (Table 1). A major change is observed between 195 and 223 K, which is consistent with the abrupt drop of the magnetic susceptibility in this temperature range. Between 133 and 195 K or between 223 and 253 K, however, the dihedral angles show no significant variation, which is again in agreement with the magnetic data.

The unusual magnetic properties of **1** can be rationalized on the basis of the crystallographic findings. While some contribution to magnetic coupling from the pyrazolate is certainly present, it is likely that the azide provides the dominant intramolecular pathway.[10] Magnetostructural correlations for $\mu_{1,3}$-azido bridged dinickel(II) complexes have revealed that two geometric parameters, namely the Ni-N-N angles and the dihedral angle, ϕ, along the azide ligand, are of major importance.[11,12] For a Ni-NNN-Ni torsion angle of $\phi = 180°$, the antiferromagnetic coupling is predicted to have a maximum at Ni-N-N angles of around 108° and to decrease at larger angles. On the other hand, the maximum coupling for all Ni-N-N angles is expected for a torsion of 180° (or 0°). In the absence of any constraining ligand scaffold, Ni-N-N angles in dinuclear complexes or 1D extended systems with a single $\mu_{1,3}$-azido bridge tend to lie in the range 115–145°, with $\phi = 140$–$180°$, thus resulting in J values in the range -17 to $-100\ \mathrm{cm}^{-1}$.[11] A particularly strong antiferromagnetic coupling of around $-100\ \mathrm{cm}^{-1}$ has been observed for some 1D chain complexes with a *trans*-{Ni-($\mu_{1,3}$-N_3)-Ni} motif featuring acute Ni-N-N angles (120.9 or 115.6/116.8°, respectively) and a large ϕ (180 or 175.5°, respectively),[11,13] or in a dinickel(II) complex with extremely obtuse Ni-N-N angles of 109.9°.[14] Similar correlations appear also to be valid for μ_3- or μ_4-azide linkages.[7]

In the case of **1** the Ni1-N3-N4 angles are quite acute and are similar at 133 K [120.7(3)°] and 253 K [116.7(3)°], whereas the torsion Ni-NNN-Ni differs dramatically [4.3(4) versus −46.6(4)°]. Given the above-mentioned magnetostructural correlations, a large antiferromagnetic intramolecular coupling of the order of almost $-100\ \mathrm{cm}^{-1}$ can thus be anticipated for the low-temperature phase (where the torsion angle is close to 0°), while a significantly diminished coupling should result from the severe tilting of the azide bridge in the high-temperature species, in accordance with the experimental

findings ($-(81\pm1.5)$ versus $-(24\pm1.0)\,cm^{-1}$). Hence, the bridging azide within the bimetallic pocket of the dinickel(II) scaffold of **1** can be viewed as a molecular on/off switch for the antiferromagnetic coupling between the two metal ions.

Close inspection of the crystallographic changes accompanying the phase transition reveals that the sulfur-bound ethyl groups of the ligand side arms of L^- are disordered about two positions above the hysteresis range (at 223 and 253 K), with temperature-dependent occupancy factors for S2-Et, whereas this disorder disappears below the hysteresis range. Concomitantly, an abrupt shrinkage of the crystallographic *a* axis upon cooling below the hysteresis range is observed, whereas the changes of the *b* and *c* axes are only minor (Table 1). As can be seen from the unit-cell plot (Figure S1 in the Supporting Information), the disordered ethyl group bound to S2 affects the stacking along the *a* axis. The abrupt shrinkage of this axis can thus be linked to the disappearance of the disorder, which apparently allows a more efficient packing of the molecules at low temperatures. However, it is still unclear at this stage how the appearance or disappearance of the disorder is coupled to the changes of the dihedral Ni-NNN-Ni angle within the bimetallic molecules.

Interestingly, a two-step behavior of the phase transition is discernible from the magnetic data. The DSC curve not only reflects the approximately 20-K hysteresis, but also this two-step behavior of the phase transition (Figure 4). Determination of the cause of this unusual feature and a more detailed analysis of the phase transition is currently under investigation.

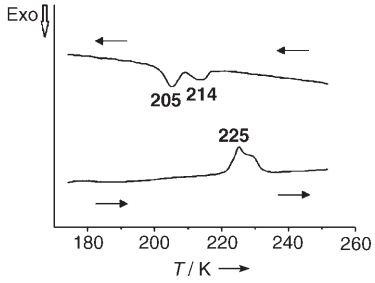

Figure 4. DSC curve for **1** showing the two-step thermal hysteresis between 205 and 230 K.

While phenomenologically reminiscent of spin-crossover behavior, the origin of the thermal magnetic bistability of **1** is fundamentally different: both metal ions retain their individual high-spin ($S=1$) state, but the bridging azide acts as a toggle switch that turns the antiferromagnetic coupling between the nickel(II) ions on or off. While phase transitions associated with small changes in magnetic properties have been observed for polymeric metal azide systems,[15] a hysteresis as distinct as that observed for **1** is unprecedented, and to the best of our knowledge this is the first case where both the high- and low-temperature phases have been characterized crystallographically to reveal the azide functioning as a well-defined molecular switch. Current work focuses on, inter alia, elucidating the cause of the two-step hysteretic behavior as well as investigating pressure effects on the magnetic bistability of **1**.

Experimental Section

Caution! Although no problems were encountered in this work, transition metal perchlorate and azide complexes are potentially explosive and should be handled with due care.

$[LNi_2(N_3)_3]$ (**1**): A solution of HL[16] (512 mg, 1.07 mmol) in methanol (65 mL) was treated with KO*t*Bu (1 equiv, 120 mg, 1.07 mmol). After stirring the mixture for 1 h at room temperature, $Ni(ClO_4)_2\cdot 6H_2O$ (2 equiv, 783 mg, 2.14 mmol) was added and the reaction mixture was stirred overnight. Any white precipitate was then removed by filtration and the resulting green solution was treated with 3.5 equiv of NaN_3 (244 mg, 3.75 mmol) and the mixture again stirred overnight. The light-green precipitate was separated by filtration and the resulting green solution was evaporated to dryness. The residue was taken up in acetone (15 mL) and layered with hexane (15 mL) to obtain green crystals of **1** (275 mg, 36%). IR (KBr): $\tilde{\nu}=$ 2965 (w), 2924 (w), 2870 (w), 2854(w), 2043 [(vs), $\nu(N_3^-)$], 1454 (w), 1418 (w), 778 (w) cm^{-1}. MS(FAB+): m/z (%) = 677 (100) $[LNi_2(N_3)_2]^+$, 635 (15) $[LNi_2(N_3)]^+$. $C_{21}H_{41}N_{13}Ni_2S_4$ (721.3): calcd.: C 34.97, H 5.73, N 25.24; found: C 35.03, H 5.75, N 24.60.

Received: June 8, 2005
Published online: October 7, 2005

Keywords: azides · bridging ligands · magnetic properties · molecular switches · nickel

[1] O. Kahn, J. P. Launay, *Chemtronics* **1988**, *3*, 140–151.
[2] J. S. Miller, *Angew. Chem.* **2003**, *115*, 27–29; *Angew. Chem. Int. Ed.* **2003**, *42*, 27–29.
[3] a) P. Gütlich, A. Hauser, H. Spiering, *Angew. Chem.* **1994**, *106*, 2109–2141; *Angew. Chem. Int. Ed. Engl.* **1994**, *33*, 2024–2054; b) O. Kahn, C. J. Martinez, *Science* **1998**, *279*, 44–48; c) O. Kahn, J. Kröber, C. Jay, *Adv. Mater.* **1992**, *4*, 718–728; d) A. Bousseksou, G. Molnár, G. Matouzenko, *Eur. J. Inorg. Chem.* **2004**, 4353–4369.
[4] a) W. Fujita, K. Awaga, *Science* **1999**, *286*, 261–262; b) W. Fujita, K. Awaga, *J. Solid State Chem.* **2001**, *159*, 451–454; c) M. E. Itkis, X. Chi, A. W. Cordes, R. C. Haddon, *Science* **2002**, *296*, 1443–1445; d) J. L. Brussom, O. P. Clements, R. C. Haddon, M. E. Itkis, A. A. Leitch, R. T. Oakley, R. W. Reed, J. F. Richardson, *J. Am. Chem. Soc.* **2004**, *126*, 14692–14693.
[5] F. L. De Panthou, D. Luneau, R. Musin, L. Öhrström, A. Grand, P. Turek, P. Rey, *Inorg. Chem.* **1996**, *35*, 3484–3491.
[6] a) J. M. Migliori, W. M. Reiff, A. M. Arif, J. S. Miller, *Inorg. Chem.* **2004**, *43*, 6875–6877; b) S. M. Humphrey, P. T. Wood, *J. Am. Chem. Soc.* **2004**, *126*, 13236–13237.
[7] a) F. Meyer, P. Kircher, H. Pritzkow, *Chem. Commun.* **2003**, 774–775; b) S. Demeshko, G. Leibeling, W. Maringgele, F. Meyer, C. Mennerich, H.-H. Klauss, H. Pritzkow, *Inorg. Chem.* **2005**, *44*, 519–528; c) F. Meyer, S. Demeshko, G. Leibeling, B. Kerstiug, E. Kaifer, H. Pritzkow, *Chem. Eur. J.* **2005**, *11*, 1518–1526.
[8] X-ray structure data: Stoe IPDS II diffractometer, ω scans, $Mo_{K\alpha}$ radiation ($\lambda=0.71093$ Å), graphite monochromator, structure solution with direct methods and refinement against F^2 (SHELX-97)[17] with anisotropic thermal parameters for all non-hydrogen atoms; for hydrogen atoms fixed isotropic thermal parameters ($U_{iso}=0.08$ Å^2) on calculated positions were used. Crystal dimensions: $0.21\times0.16\times0.12$ mm^3, orthorhombic, space group *Pbcn* (no. 60), $Z=4$, $F(000)=1512$. At 223 and 253 K the sulfur-bound ethyl groups are disordered about two positions with temperature-dependent occupancy factors (S1-Et at 253 K: 0.46(7)/0.54(7); at 223 K: 0.46(8)/0.54(8). S2-Et at 253 K: 0.766(9)/0.234(9); at 223 K: 0.836(10)/0.164(10)). For the disordered parts, DFIX restraints were applied for the S–C

(1.81 Å) and C–C (1.51 Å) distances, with DELU and SIMU restraints for refinement with anisotropic displacement parameters. Data collection at 133 K: $a = 15.9739(12)$, $b = 8.6167(8)$, $c = 22.8983(17)$ Å, $V = 3151.8(4)$ Å^3, $\rho_{calcd} = 1.520$ kg m^{-3}, $\mu = 1.496$ mm^{-1}, $3.6 \le 2\theta \le 49.4°$, $-18 \le h \le 18$, $-10 \le k \le 9$, $-24 \le l \le 26$, 13945 data collected, 2679 unique data ($R_{int} = 0.0647$), 2123 data with $I > 2\sigma(I)$, 184 refined parameters, GOF(F^2) = 1.057, final R indices: $R1 = 0.0368$ (0.0556 all data), $wR2 = 0.0680$ (0.0731 all data), max./min. residual electron density: 0.365/−0.427 e Å^{-3}. Data collection at 195 K: $a = 16.0886(12)$, $b = 8.6241(8)$, $c = 22.9437(16)$ Å, $V = 3183.4(4)$ Å^3, $\rho_{calcd} = 1.505$ kg m^{-3}, $\mu = 1.481$ mm^{-1}, $3.6 \le 2\theta \le 49.4°$, $-18 \le h \le 18$, $-10 \le k \le 9$, $-24 \le l \le 26$, 14216 data collected, 2706 unique data ($R_{int} = 0.0745$), 2031 data with $I > 2\sigma(I)$, 184 refined parameters, GOF(F^2) = 1.092, final R indices: $R1 = 0.0422$ (0.0672 all data), $wR2 = 0.0780$ (0.0848 all data), max./min. residual electron density: 0.465/−0.280 e Å^{-3}. Data collection at 223 K: $a = 16.3424(12)$, $b = 8.6933(8)$, $c = 22.9634(15)$ Å, $V = 3262.4(4)$ Å^3, $\rho_{calcd} = 1.469$ kg m^{-3}, $\mu = 1.446$ mm^{-1}, $3.5 \le 2\theta \le 49.6°$, $-19 \le h \le 19$, $-9 \le k \le 10$, $-26 \le l \le 24$, 14688 data collected, 2784 unique data ($R_{int} = 0.0752$), 2016 data with $I > 2\sigma(I)$, 220 refined parameters, GOF(F^2) = 1.060, final R indices: $R1 = 0.0437$ (0.0728 all data), $wR2 = 0.0748$ (0.0826 all data), max./min. residual electron density: 0.344/−0.228 e Å^{-3}. Data collection at 253 K: $a = 16.3677(10)$, $b = 8.7169(7)$, $c = 22.9876(13)$ Å, $V = 3279.8(4)$ Å^3, $\rho_{calcd} = 1.461$ kg m^{-3}, $\mu = 1.438$ mm^{-1}, $3.5 \le 2\theta \le 49.7°$, $-19 \le h \le 19$, $-10 \le k \le 10$, $-24 \le l \le 27$, 19079 data collected, 2838 unique data ($R_{int} = 0.0706$), 2045 data with $I > 2\sigma(I)$, 220 refined parameters, GOF(F^2) = 1.019, final R indices: $R1 = 0.0370$ (0.0614 all data), $wR2 = 0.0729$ (0.0804 all data), max./min. residual electron density: 0.260/−0.230 e Å^{-3}. CCDC-271898 (133 K), -271899 (195 K), -271900 (223 K), and -271901 (253 K) contain the supplementary crystallographic data for this paper. These data can be obtained free of charge from the Cambridge Crystallographic Data Centre via www.ccdc.cam.ac.uk/data_request/cif.

[9] Parameters obtained for data above 230 K should be interpreted with care because of the limited temperature range available for the fitting procedure.

[10] a) M. Konrad, F. Meyer, A. Jacobi, P. Kircher, P. Rutsch, L. Zsolnai, *Inorg. Chem.* **1999**, *38*, 4559 – 4566; b) G. Leibeling, S. Demeshko, B. Bauer-Siebenlist, F. Meyer, H. Pritzkow, *Eur. J. Inorg. Chem.* **2004**, 2413 – 2420.

[11] J. Ribas, A. Escuer, M. Monfort, R. Vicente, R. Cortés, L. Lezama, T. Rojo, *Coord. Chem. Rev.* **1999**, *193–195*, 1027 – 1068, and references therein.

[12] F. Meyer, H. Kozlowski in *Comprehensive Coordination Chemistry II, Vol. 6* (Eds.: J. A. McCleverty, T. J. Meyer), Pergamon, **2004**, pp. 247 – 554.

[13] R. Vicente, A. Escuer, J. Ribas, M. S. El Fallah, X. Solans, M. Font-Bardia, *Inorg. Chem.* **1995**, *34*, 1278 – 1281.

[14] J. Hausmann, M. H. Klingele, V. Lozan, G. Steinfeld, D. Siebert, Y. Journaux, J. J. Girerd, B. Kersting, *Chem. Eur. J.* **2004**, *10*, 1716 – 1728.

[15] a) A. Escuer, R. Vicente, J. Ribas, X. Solans, *Inorg. Chem.* **1995**, *34*, 1793 – 1798; b) M. Monfort, J. Ribas, X. Solans, M. Font-Bardia, *Inorg. Chem.* **1996**, *35*, 7633 – 7638; c) F. A. Mautner, R. Cortés, L. Lezama, T. Rojo, *Angew. Chem.* **1996**, *108*, 96 – 98; *Angew. Chem. Int. Ed. Engl.* **1996**, *35*, 78 – 80.

[16] M. Konrad, F. Meyer, K. Heinze, L. Zsolnai, *J. Chem. Soc. Dalton Trans.* **1998**, 199 – 205.

[17] G. M. Sheldrick, SHELXL-97, Program for Crystal Structure Refinement, University of Göttingen, Göttingen (Germany), **1997**; G. M. Sheldrick, SHELXS-97, Program for Crystal Structure Solution, University of Göttingen, Göttingen (Germany), **1997**.

